Entropy **2010**, *12*, 1484-1498; doi:10.3390/e12061484

OPEN ACCESS

entropy

ISSN 1099-4300

www.mdpi.com/journal/entropy

Article

Prediction of Droplet Size and Velocity Distribution in Droplet Formation Region of Liquid Spray

Ehsan Movahednejad[1], Fathollah Ommi[2,]* and S. Mostafa Hosseinalipour[3]

[1] Engineering Faculty, Tarbiat Modares University, 14115-143, Tehran, Iran; E-Mail: movahed@modares.ac.ir

[2] Engineering Faculty, Tarbiat Modares University, 14115-143, Tehran, Iran

[3] Iran University of Science and Technology, Tehran, Iran; E-Mail: alipour@iust.ac.ir

† Present address: University of Alabama in Huntsville, AL 35899, USA.

* Author to whom correspondence should be addressed; E-Mail: fommi@modares.ac.ir; Tel.: +98-21-82883948; Fax: +98-21-88005040.

Received: 12 April 2010 / Accepted: 20 May 2010 / Published: 10 June 2010

Abstract: Determining the distributions of size and velocity of droplets formed at the end of primary breakup region is followed in this paper. The droplet formation stage at the end of primary breakup is random and stochastic and it can be modeled by statistical means based on the maximum entropy principle (MEP). The MEP formulation predicts the atomization process while satisfying constraint equations based on conservations of mass, momentum and energy. This model is capable of considering drag force on produced droplets through gas-liquid interaction using new approach. The model prediction is compared favorably with the experimentally measured size and velocity distributions of droplets for sprays produced by the two nozzles of considerably different geometries and shows satisfactory agreement.

Keywords: maximum entropy; spray; droplet; size-velocity distribution; probability

PACS Codes: 47.55.-t

List of notations

$\dot{n}$	Total number of droplets being produced per unit time
S_m	dimensionless mass source term
S_{mu}	dimensionless momentum source
S_e	Energy source term
$\dot{m}_o$	mass flow rate
$\dot{J}_O$	Momentum flow rate
$\dot{E}_O$	Energy flow rate
λ_i	Lagrange coefficient
C_D	Droplets drag coefficient
C_f	Drag coefficient over the liquid sheet
D_{30}	Mass mean diameter
D_i	diameter of i_{th} droplet
f	probability density function
H	Shape factor for velocity profile
K	Boltzmann constant
N	normalized cumulative droplet number
p_i	probability of occurrence of state i
u	Droplet velocity
U_0	Mean velocity of jet in nozzle outlet
U_m	Droplets mean velocity
V_i	Volume of i_{th} droplet
V_m	Mean volume of droplet
We	Weber number

1. Introduction

The distribution of droplet size and velocity in sprays is a crucial parameter needed for fundamental analysis of practical spray systems. Detailed information regarding droplet size and velocity distributions in sprays is of ultimate importance for the design, operation, and optimization of spray systems [1]. Specification of droplet size and velocity distributions in the immediate downstream of spray is also essential as boundary conditions for advanced computational fluid dynamics (CFD) based two-phase spray transport calculations [2,3]. Classic models to predict diameter and velocity distribution of droplets were derived mainly from experimental data. In this procedure, a curve is fitted on different data is obtained from various conditions of nozzle operations. This procedure is the main basis for distributions such as the Rosin-Rambler, Nukiyama-Tanasawa and log-kernel distributions, *etc.* [4,5].

Several studies have attempted to derive more general droplet size-velocity distribution based on statistical approaches [4,6]. Since mid-1980s, the Maximum Entropy Principle (MEP) method has gained popularity in the field of atomization and sprays to predict droplet size and velocity distribution and has obtained reasonable success. The MEP approach can predict the most likely droplet size and

velocity distributions under a set of constraints expressing the available information related to the distribution sought. The application of MEP to spray modeling was pioneered by Sellens and Brzustowski [7] and Li and Tankin [8]. This approach assumes that in addition to conservation of mass, momentum and energy, the droplet size distribution function satisfies a maximum entropy principle. This approach suggests the most probable size distribution in which conservation equations are satisfied while system entropy is maximized.

Other investigators have implemented and further developed this method. Ahmadi and Sellens [9] reached the conclusion that prediction of the droplet size distribution was independent of the velocity distribution and the constraints on momentum and kinetic energy carried only velocity information. Cousin *et al.* [10] advocated a new approach in which the constraint is based on a single representative diameter instead of the commonly used conservation laws. Most previous works considered the droplets just upon jet breakup and neglect the drag force of air on droplets in the first part of jet breakup. Sellens and Brzustowski [11] and Li *et al.* [12], in different works, used a simplified drag formulation to propagate the velocity distribution downstream through a gas field using mechanic of droplets. In this paper, a method is used to account for drag force on produced droplets at the final stage of the drop formation region and the resulting size and velocity distributions of droplets, by recalculating the momentum constrain source term. What's new in this paper compared to the work of other groups by Sellens *et al.* in references [7,9,11] and Li *et al.* in references [8,12] is the extension of MEP to include momentum transfer between new formed droplets and surrounding gas after the sheet breakup regime to beginning of secondary breakup region and before the region where the effects of turbulence, collision and coalescence effect the formation and distribution of droplets. Comparison between the model prediction and available experimental data indicates good agreement between the two.

2. Mathematical Model and Governing Equations

To extract governing equations and to determine size and velocity distribution for particles, a control volume is considered from the outlet of the injector to the droplet formation location where the droplets form from ligaments.

The droplet formation process in the control volume can be considered as a transformation from one to another equilibrium state. According to the thermodynamics laws, during a changing in a state the mass, momentum and energy are conserved while entropy maximization occurs. Regarding the formulation of entropy maximization, the conservation equation can be stated in terms of the joint probability density function: p_{ij}, which is the probability of finding a droplet with volume V_i and velocity u_j. Hence, the mass, momentum and energy conservation equation can be restated as:

Mass balance:
$$\sum_i \sum_j p_{ij} V_i \rho \dot{n} = \dot{m}_o + S_m \tag{1}$$

Momentum balance:
$$\sum_i \sum_j p_{ij} V_i \rho \dot{n} u_j = \dot{J}_o + S_{mu} \tag{2}$$

Energy balance:
$$\sum_i \sum_j p_{ij} \dot{n} (V_i \rho u_j^{\,2} + 2\sigma A_i) = \dot{E}_o + S_e \tag{3}$$

In these equations, $\dot{n}$ is the droplet generation rate in the spray. $\dot{m}_o$ ، $\dot{J}_O$ ، $\dot{E}_O$ are mass flow rate, momentum and energy which enter the control volume from the injector outlet. S_m, S_{mu} and S_e are the source terms for mass, momentum and energy equations, respectively.

In addition to the kinetic energy, a droplet has a surface energy, which is necessary for its formation. Therefore, $2\sigma A_i$ terms are considered in the energy equation. To obtain a more proper form of these equations, it is possible to normalize the equation with $\dot{m}_o$ ، $\dot{J}_O$ ، $\dot{E}_O$. Utilizing the definition of averaged velocity (U_0) and droplet-averaged volume (V_m) in the spray, mass, momentum and energy equations can be rewritten.

In addition to the three above mentioned equations, according to the probability concept, total summation of probabilities should be equal to unity:

$$\sum_i \sum_j p_{ij} = 1 \tag{4}$$

As mentioned before, there is infinite number of probabilities p_{ij} which satisfy equations (1) to (4); therefore, the most appropriate distribution is the one in which Shannon entropy is maximized [13]:

$$S = -K \sum_i \sum_j p_{ij} \ln p_{ij} \tag{5}$$

where K is the Boltzmann's constant. Using the Lagrangian multiplier method, the probability of finding the droplets with volume between $\overline{V}_{n-1}$ and $\overline{V}_n$, and velocity between $\overline{u}_{m-1}$ and $\overline{u}_m$ while entropy is maximized is:

$$\sum_{\overline{V}_{n-1}} \sum_{\overline{u}_{m-1}} p_{ij} = \sum_{\overline{V}_{n-1}}^{\overline{V}_n} \sum_{\overline{u}_{m-1}}^{\overline{u}_m} \exp[-\lambda_0 - \lambda_1 \overline{V}_i - \lambda_2 \overline{V}_i \overline{u}_j - \lambda_3 (\frac{\overline{V}_i \overline{u}_j^2}{H} + \frac{B' k_i \overline{V}_i}{H})]$$
$$B' = \frac{2\sigma}{\rho U_0^2} \tag{6}$$

where the set of λ_i is a collection of arbitrary Lagrange multipliers which must be evaluated for each particular solution. To obtain the coefficient λ_i , equations (1) to (4) and (6) should be solved simultaneously. According to Li and Tankin model [8] it is also feasible to convert the analytical domain from volume and velocity of droplets to their diameter and velocity. Hence, the formulation can be written according to the probability of finding droplets which their diameters are between $\overline{D}_{n-1}$ and $\overline{D}_n$ and their velocities are between $\overline{u}_{m-1}$ and $\overline{u}_m$. Although as discussed by Dumouchel [14,15], such a procedure is inconsistent with the MEF mathematical manipulation and must be prohibited without taking the appropriate precaution to ensure entropy invariance.

Generally, in the atomization problems, the size and velocity of droplets are varied continuously and the equations can be stated in the integral form over the size and velocity of droplet. So the continuous probability density function (PDF) f is used for the size and velocity of droplets. Thus:

$$f = 3\overline{D}^2 \exp[-\lambda_0 - \lambda_1 \overline{D}^3 - \lambda_2 \overline{D}^3 \overline{u} - \lambda_3 (\frac{\overline{D}^3 \overline{u}^2}{H} + \frac{B\overline{D}^2}{H})]$$
$$We = \frac{\rho U_0^2 D_{30}}{\sigma}, \; B = \frac{12}{We} \tag{7}$$

Droplets generated from spraying are relatively small and usually their shape is considered to be spherical due to the surface tension effects. Equations (1) to (4) and (6) can be restated in the integral form within the analytical domains of the velocity and diameter of droplet. Hence, regarding above mentioned statement, to obtain Lagrange coefficient (λ_i) in PDF (*f*), it is necessary to solve the following normalized set of equations [8,12]:

$$\begin{cases} \int_{\overline{D}_{\min}}^{\overline{D}_{\max}} \int_{\overline{u}_{\min}}^{\overline{u}_{\max}} f\overline{D}^3 d\overline{u} d\overline{D} = 1 + \overline{S}_m \\ \int_{\overline{D}_{\min}}^{\overline{D}_{\max}} \int_{\overline{u}_{\min}}^{\overline{u}_{\max}} f\overline{D}^3 \overline{u} d\overline{u} d\overline{D} = 1 + \overline{S}_{mu} \\ \int_{\overline{D}_{\min}}^{\overline{D}_{\max}} \int_{\overline{u}_{\min}}^{\overline{u}_{\max}} f(\frac{\overline{D}^3 \overline{u}^2}{H} + \frac{B\overline{D}^2}{H}) d\overline{u} d\overline{D} = 1 + \overline{S}_e \\ \int_{\overline{D}_{\min}}^{\overline{D}_{\max}} \int_{\overline{u}_{\min}}^{\overline{u}_{\max}} f d\overline{u} d\overline{D} = 1 \\ f = 3\overline{D}^2 \exp[-\lambda_0 - \lambda_1 \overline{D}^3 - \lambda_2 \overline{D}^3 \overline{u} - \lambda_3 (\frac{\overline{D}^3 \overline{u}^2}{H} + \frac{B\overline{D}^2}{H}) \end{cases} \tag{8}$$

In these equations diameter, velocity and dimensionless source terms are described as: $\overline{D}_i = D_i / D_{30}$, $\overline{u}_j = u_j / U_0$, $\overline{S}_m = S_m / \dot{m}_o$, $\overline{S}_{mu} = S_{mu} / \dot{J}_O$, $\overline{S}_e = S_e / \dot{E}_O$.

H is the shape factor for the velocity profile and is defined as:

$$H = \left(\frac{\dot{E}_O}{\dot{m}_o} \right) \Big/ U_0^2 = \left(\frac{\dot{E}_O}{\dot{m}_o} \right) \Big/ \left(\frac{\dot{J}_O}{\dot{m}_o} \right)^2 \tag{9}$$

When the outlet velocity profile is uniform, the shape factor (*H*) is equal to 1. As it can be seen from the equations, the solution domains are changed from $\overline{D}_{\min}$ to $\overline{D}_{\max}$ and from $\overline{u}_{\min}$ to $\overline{u}_{\max}$ .The variations of $\overline{D}$ and $\overline{u}$ in the domain are independent, so the probability of existence for every droplet is considered with arbitrary velocity $\overline{u}$ and diameter $\overline{D}$.

In this work the mass source term is neglected, which indicates ion turn that the evaporation and distillation of liquid during the spraying process are neglected. Also in the present formulation, all the sources of energy like kinematic energy, surface energy and turbulence energy will be accumulated in the energy source term (*Se*). If there is any energy conversion within the control volume, it is not considered as a source term. For instance, the energy conversion from heat and the energy exchange from evaporation and distillation can be pointed out. Within the control volume, there is a momentum exchange between the liquid flow and the gas. This momentum transformation should be considered as a momentum source term to account for the drag force on liquid body.

To obtain this function, it is imperative to determine the Lagrange multipliers λ_i in equations (7) which can be computed from solving the equation set (8) simultaneously. In this paper, to solve this set of equation, the Newton-Raphson method was used. At first, some initial value for the $\lambda_0, \lambda_1, \lambda_2, \lambda_3$ was assumed. Then, using these values and the Newton-Raphson procedure, new value for λ_0 and then $\lambda_1, \lambda_2, \lambda_3$ was computed and this procedure continued until final answer was obtained. It is noted that functions in equation set (8) and their derivatives are integral functions. Therefore, double integrals function should be solved numerically for all iterations. Another important point is that integral

functions and the terms in these integrals are exponential; hence, if the selection of an initial guessed of λ_i turns out to be not enough close to the answer, the solution will not converge to the answer.

3. Modeling

To assess the maximum entropy principle for determination of PDF, the procedure is evaluated for two different sprays; a spray resulting from a hollow cone nozzle and a spray from an industrial gas turbine nozzle.

The first condition is the one which was previously used by Li *et al.* [12]. The spray characteristics are presented in Table 1. To solve the governing equations, analytical domains for non dimensional diameter and velocity are considered from 0 to 3. If the velocity profile at the injector outlet is assumed uniform, the shape factor of velocity profile (H) will be unity. But if the outlet flow from the injector is assumed to be fully developed and turbulent, this factor will be equal to 1.01647. So the shape factor will be between 1 and 1.01647 for the relatively developed fluid [16].

Table 1. Spray characteristics [12].

Liquid Density	Surface Tension	Ambient Pressure	Gas Density	Flow rate	Liquid Average Velocity	D_{30}
998.2 (Kg/m^3)	0.0736 (N/m)	1 atm	1.22 (Kg/m^3)	$2.809*10^{-3}$ (Kg/s)	40.8 (m/s)	$1.37*10^{-5}$ (m)

The control volume extends from the nozzle exit to the sheet breakup region. It is important to note that this region is different from the droplet formation region. The momentum source term is obtained by considering the drag force acting on the liquid sheet due to the relative motion of the gas phase over the breakup length. The analysis was carried out assuming that the flat plate of liquid sheet was fixed and the gas phase velocity above the liquid-sheet boundary layer was taken as mean liquid velocity at the nozzle outlet. The drag force on both sides of the liquid sheet is written as [17]:

$$F = 2[\frac{1}{2}\rho_g (U_g - U_0)^2 A C_f)]$$
$$C_f = \frac{1.328}{\sqrt{\mathrm{Re}_g}} \qquad \mathrm{Re}_g \le 10^5 \tag{10}$$

where C_f is the drag coefficient for flow over a flat liquid plate with contact area of A, which has different values for laminar and turbulent flows.

The drag force is equal to the amount of momentum transferred from the surrounding gas medium to the liquid sheet per unit time. Therefore, the momentum source term is obtained as:

$$\bar{S}_{mu} = \frac{F}{\dot{J}_m} = \frac{F}{\rho_l U_0^{\,2} A_{cross}} = \frac{\rho_g}{\rho_l}(\frac{U_g}{U_0} - 1)^2 C_f (\frac{L_b}{h}) \tag{11}$$

Where, L_b and h are breakup length and thickness of the liquid sheet and A_{cross} shows it's cross section area. Considering a laminar boundary layer flow passing on a flat plate, C_f is computed; so the

momentum source term can be evaluated as shown in Table 2. The Reynolds number is based on the jet velocity at the outlet of injector [12].

Table 2. Computed drag force and source term for momentum equation.

Weber Number	Reynolds Number	Drag Force	Momentum flow rate to Control volume	Non-dimensional Momentum source term
W_e	Re	F (N)	$\dot{J}_O$	$\bar{S}_{mu}$
311	18200	$1.953*10^{-3}$	0.1147	-0.01702

Figure 1 shows the probability contour of size and velocity of a hollow-cone spray in a pre-filming atomizer. Model results are shown in Figure 1-a while experimental data of Li *et al.* [12] are presented in Figure 1b.

This representation allows the observation of the most striking features of the joint distribution. The relationship and inter-dependence between the size and the velocity of the sprayed droplets are quite evident in Figure 1. The difference between contours is affected by measurement accuracy for the momentum source term, which is also affected by the drag force exerted on droplets after jet breakup. Because the velocity and size of droplets are measured at the small distance from the breakup regime and during this interval, drag force exerted on the droplets that are generated from the liquid jet are not considered in the present model. In Figure 2, the measured and computed probability distributions of droplet's size are demonstrated. This function is acquired from the integration of velocity-size probability distribution function over the velocity interval. As apparent from the figure, there is a satisfactory agreement between the theoretical and experimental results.

As another comparison, the present model is compared with the test results of an actual gas turbine nozzle (PWC nozzle) provided by Mitra [18]. The PWC nozzle produces an annular liquid sheet at the nozzle exit with air flow both inside and outside the liquid sheet. Experimentally measured spray characteristics at the nozzle exit as well as the estimated momentum source term are provided in Table 3. The momentum source term calculated using equation (11) and the solution domains for $\overline{D}$ and $\overline{u}$ are considered from 0 to 2.5. The measurement reported by Mitra *et al.* [18,19] was carried out at the centerline located 5 mm downstream from nozzle exit in vicinity of droplet formation position. Figure 3 shows the comparison between the theoretical and the experimental distributions. It is observed that the droplet size distribution over predicts for smaller droplet diameters.

This problem has also been reported by Dumouchel [15] and Sirignano and Mehring [20]. However, for droplet diameter greater than 30 microns, the theoretical prediction matches better with the experimental distribution. The above comparisons show that the present model can predict initial droplet size and velocity distributions reasonably well for sprays produced by two nozzles with considerably different geometries.

Figure 1. Comparison of theoretical and experimental contour.

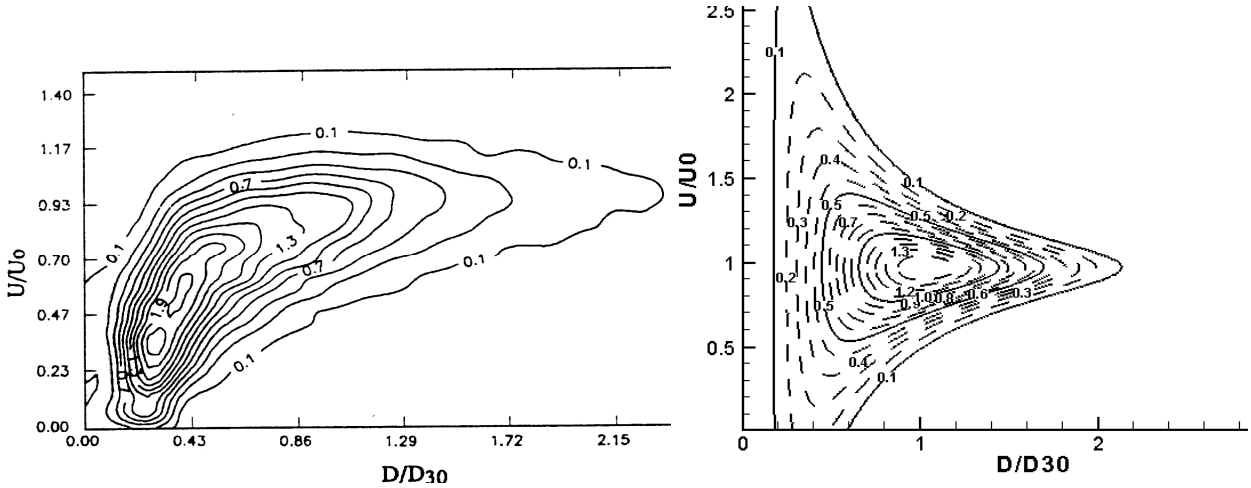

a. The predicted probability contour. b. The measured probability contour [12].

Figure 2. Comparison of theoretical (solid line) and experimental (dashed line) [12] droplet size distribution.

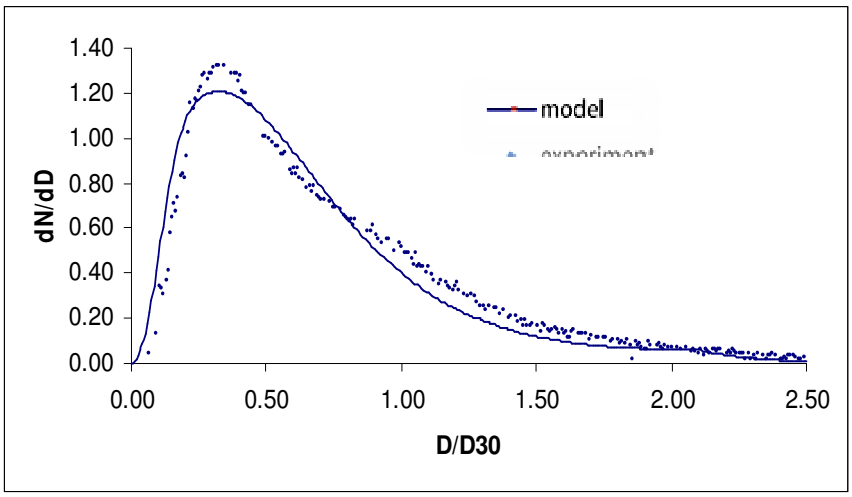

Table 3. Spray characteristics and source terms for PWC nozzle.

Experiment				Calculation			
U_0 (m/s)	Ug (m/s)	Breakup Length (mm)	D_{30}(micron)	Re_g	Drag Coefficient (C_f)	S_{mu}	S_m
4.6	56	4	45	11420	0.0124	0.047	0.0

Figure 3. Comparison between the theoretical (MEP) and experimental (Mitra [18]) droplet size distribution for PWC nozzle.

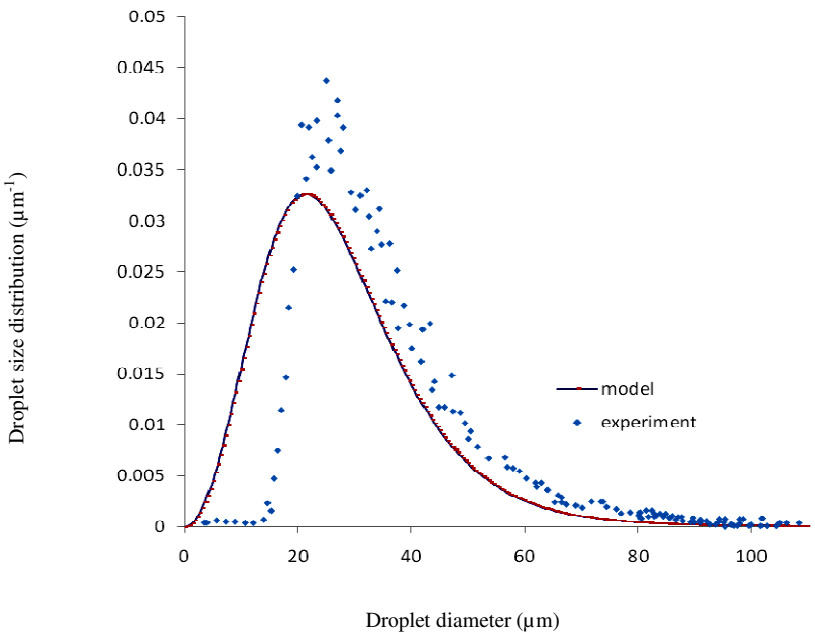

4. Modeling of Droplets Formation Region

In the previous simulation, the effects of drag force from gas stream on droplets downstream of the spray were not considered. The results belong to the beginning part of primary breakup once droplets form from ligament breakup.

One of the occasions in which momentum exchanges between the liquid and the continuous phase occurs is the influence of drag force on the droplet body. Therefore, to consider drag force on droplets, the momentum source term should be modified. This work was carried out to show a trend, rather than specific quantitative results and the downstream velocity model is drastically simplified. The gas velocity is taken to be uniform and constant. The spray is assumed to be diluted, so the collisions of droplets may be neglected. Without any collision effects the measures of the behavior of the droplets collectively will simply be the sum of the measures of behavior of the individual droplets. Figure 4 shows the control volume used for simulation and the regime in which small droplets formed at the final part of primary breakup zone, where droplets form by breakup of ligaments and mother droplets. Furthermore, in the secondary breakup zone the phenomena like turbulence, collision and coalescence effect the formation and distribution of droplets.

For this approach, the first thing required is a model for the effect of the gas field on a single droplet and all droplets are supposed to have spherical shape. To accomplish this, the velocity distribution that is predicted from modeling results is used as the initial distribution of droplets. Then drag force on individual droplets are measured (R in Equation 12). This arises out of a simple drag relation [16]:

$$R = \tfrac{1}{2} C_D \rho_a U_r^{\,2} A = C_D \frac{\rho_a \pi U_r^2 D^2}{8} \tag{12}$$

where U_r is the relative velocity and C_D is the drag coefficient evaluated from following relation [21].

$$\begin{aligned} &\mathrm{Re} \le 0.2 && C_D = 24/\mathrm{Re} \\ &0.2 \le \mathrm{Re} \le 500 && C_D = 18.5/\mathrm{Re}^{0.6} \\ &500 \le \mathrm{Re} \le 10^5 && C_D = 0.44 \end{aligned} \tag{13}$$

Figure 4. Atomization regions of the spray from the hollow cone nozzle [22].

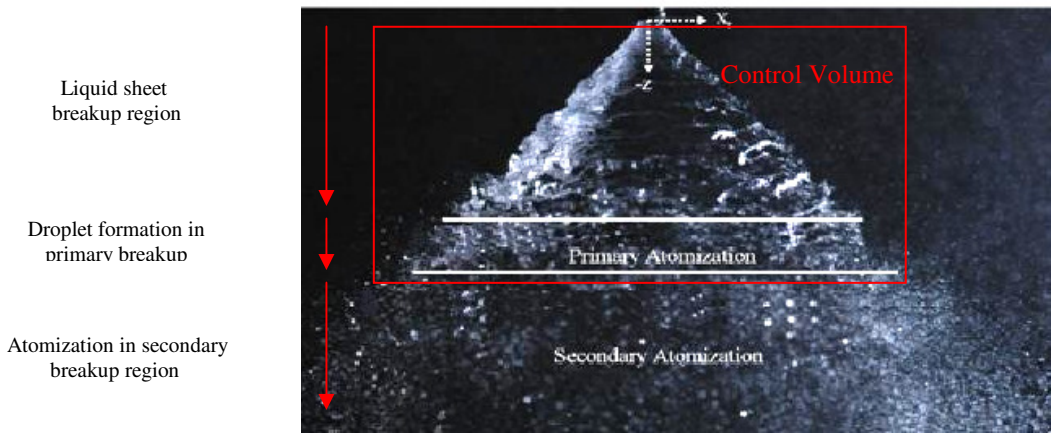

The droplets passing any point will not share the same starting time from the nozzle, but for steady flow they will have experienced the same intermediate conditions. Thus the starting time will be immaterial assuming the steady spray system. Considering the probability distribution function of droplets (f) from MEP, the number distribution of droplets for different size and velocity category is known. The velocity distribution predicted from modeling is also used as the initial distribution of droplets. Now, the drag force on each category of drop size or velocity can be computed. Using the sum of the drag forces on individual droplets, the new momentum source term can be extracted. The new momentum source term is used in the set of conservation equations and by resolving the model, the new distributions for size and velocity of droplets are gained.

The mean volumetric diameter and mean velocity of droplets can be estimated from the formulas below [23]:

$$\begin{aligned} &\overline{D}_{30}^3 = (\sum \overline{D}_{30\,j}^3)/n_u \\ &\sum \overline{D}_{30\,j}^3 = \sum_{j=1}^{j=nu} \{D_{30\,j}^3/(dN/dU)_j\} = \int fD^3 dD / \int fdD \end{aligned} \tag{14}$$

$$\begin{aligned} &\overline{U}_m = (\sum \overline{U}_{m\,i})/n_d \\ &\sum \overline{U}_{m\,i} = \sum_{i=1}^{i=nd} \{U(D)_i/(dN/dD)_i\} = \int fUdU / \int fdU \end{aligned} \tag{15}$$

where, n_u and n_d show the number of intervals on velocity and size domains respectively. The modification of the momentum source term continues until the results converge to the unique answer, as seen in Figure 5. The final droplet's size and velocity distributions belong to the droplets formed at downstream of jet breakup regime or final stage of primary breakup. Before this stage the instabilities on liquid jet and aerodynamic forces have the most important effect on the droplet formation process. After it, in the next stage (secondary breakup) turbulence plays a more significant role in droplet's

breakup. Without considering any turbulence effect (as in the present model), the drag force on droplets is only capable of modeling droplet formation to certain drop characteristics, where a steady condition established on droplet formation process, so the distribution of droplet characteristics converges to certain solution.

5. Results and Discussion

According to the previously discussed method the maximum entropy formalism was used several times to estimate probability distribution function of droplets precisely. In each step the momentum source term was modified according to drag force on new droplet formation. For the special case presented in Table 1, four steps were performed and the results have been shown in Table 4.

Figures 5 and 6 also show droplet size and velocity distributions in different steps. According to the diagram, droplet size and velocity distributions converge to the unique result that belongs to the end part of primary breakup, where there is a steady condition in droplet formation and droplet distribution in spray.

Table 4. Maximum entropy formalism results with refined momentum source terms.

Parameter	Step 1	Step 2	Step 3	Step 4
λ_1	-1.4491	-0.0393	0.0547	0.0625
λ_2	62.5777	11.1397	9.3288	9.1889
λ_3	-128.727	-22.5275	-18.7530	-18.4611
λ_4	65.4985	11.7133	9.7962	9.6479
D_{30}	0.929286	0.741426	0.72169	0.72
U_m	0.285355	0.244805	0.2468	0.247
$S_{mu}(droplets)$	0	-0.01858	-0.0036	-0.00033
$S_{mu}(drop+sheet)$	-0.0172	-0.0 3558	-0.0391	-0.0395

According to Figures 5 and 6, an increase in droplet formation through spray downstream causes an an increase in the drag force on droplets, so the distribution curves of droplets' velocity and size become more flat and its maximum value decreases. Hence, droplet size and velocity distributions become more uniform.

As a proof for the mentioned result, the experimental data of PWC has been used. In case of the PWC nozzle, measurements near the breakup location for certain flow characteristics were shown in Figure 5. Mitra [18] reported experimental results of PWC nozzle for different flow conditions on the nozzle exit.

Figure 5. Number density of droplets *versus* dimensionless droplet size.

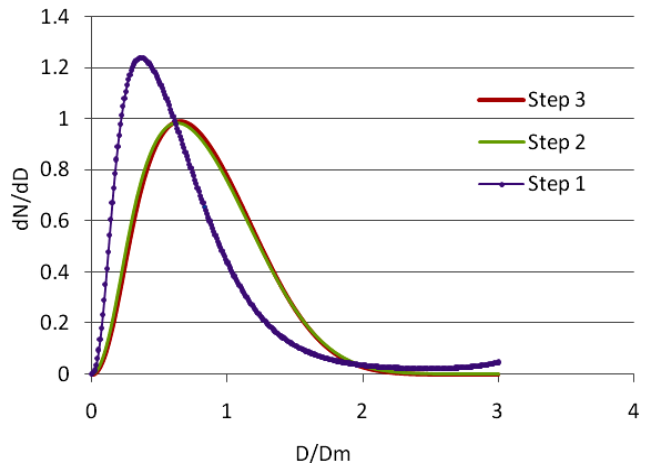

Figure 6. Number density of droplets *versus* dimensionless droplet velocity.

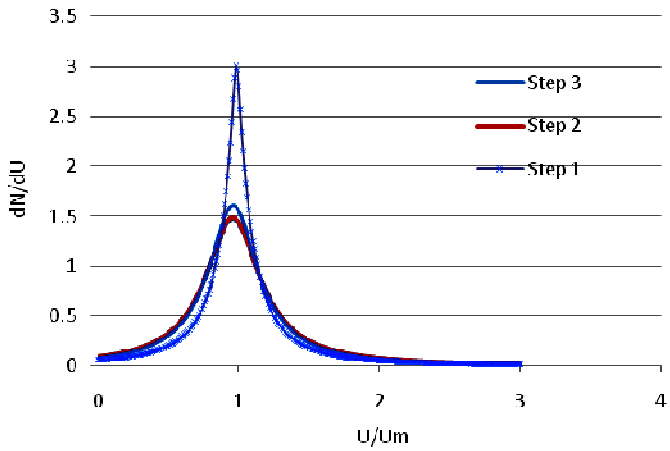

In Figure 7 the dimensional drop size distribution for downstream measurements 10 mm and 5 mm from the nozzle exit have been shown. Flow constants and inlet conditions for both measurements are the same, except gas velocity (gas velocity for measurement in 5 mm is 20% greater than the case 10 mm). Breakup length is 4 mm, so it is still expected that 10 mm from nozzle is downstream of the breakup region. Therefore, these data have been used to investigate the droplets' distribution downstream of breakup position using a comparison of results for two different positions, 5mm and 10mm from the nozzle exit.

As seen in Figure 7, at greater distance from the breakup position the population of droplets for different droplet diameters is more homogenous and has less maximum value. The same result has been attained from modeling using modified MEP. Data presented in Table 3 are used as input data, whereas, mean velocity of liquid sheet and surrounding gas as well as mean drop size provided by experiment of Mitra [18]. The droplet size distribution for the PWC nozzle using the MEP model has been shown in Figure 8. Figure 8 indicates the sensitivity of size distribution of droplets on drag force applied on droplets that is shown by source of momentum. With an increase in momentum source term that is the result of moving through down-stream of the spray, the peak of size distribution decrease and moves to bigger drop sizes. On the other hand, one can see that the size distribution of droplets

tends to be broader as going far from nozzle exit. Comparison of Figures 7 and 8 shows the agreement between experimental and theoretical results. The goal of the comparison is more showing the trends rather than competitive exact data. It is observed that the theoretical distribution in 10 mm downstream direction (Figure 8) predicts slightly greater values for big droplets compared to the experimental distribution (Figure 7). The over-prediction may be understandable because the present measurements are made at a location slightly downstream of the breakup region, where the turbulence effect which causes faster breakup might be significant; whereas, the MEP model could not see this effect.

Figure 7. Droplet size distribution of PWC nozzle for two different positions in downstream direction [18].

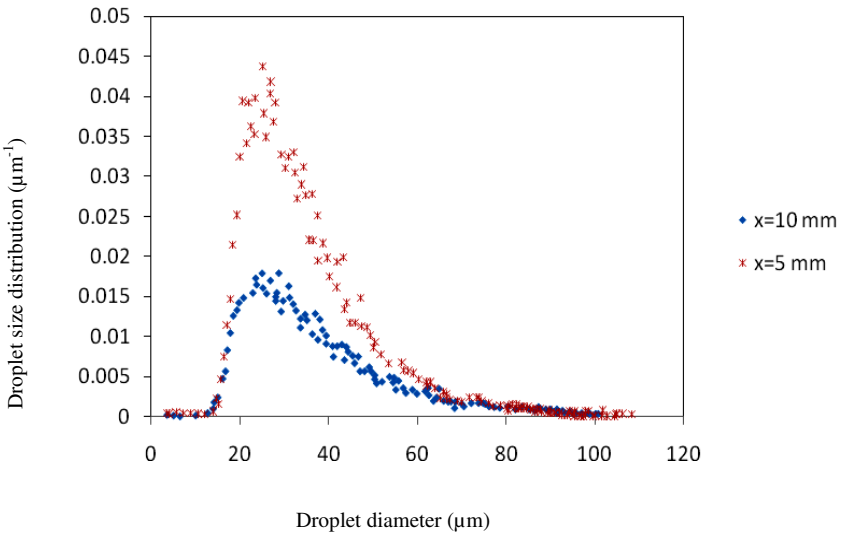

Figure 8. Prediction of droplet size distribution of PWC nozzle using MEP model for two different positions in downstream direction.

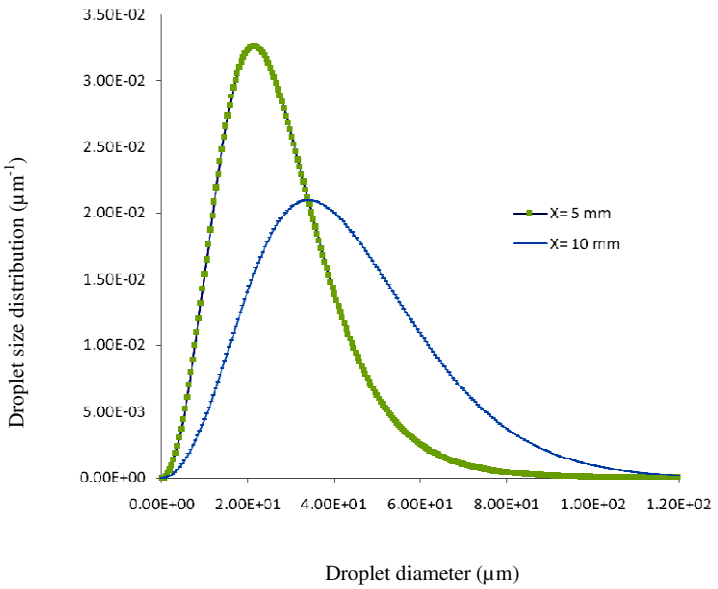

6. Conclusions

In the present paper, the random process of distributing diameter and velocity of the droplets at the final stage of droplet formation in primary breakup region is modeled implementing maximum entropy principle (MEP). This approach is applicable for predicting the size and velocity distribution of droplets in the systems in which thermodynamic equilibrium prevails. However, the process of spray formation is irreversible and not adiabatic, and there is always interaction between atomized liquid and surrounding gas. Therefore, establishing a harmony between the results of modeling using MEP and experimental data is a difficult achievement. Although simplified assumptions were used to solve the equations, the results demonstrated a satisfactory conformity with the experiments, which revealed the model's ability to account the effects of processes that occur in the spray control volume. Since the functions and their derivatives in the governing equations are in the integral and exponential form, the solution is sensitive to the initial guess λ_i and by using a wrong initial value, and the solution diverged immediately.

A precise estimation of the source terms is very important; so to acquire exact results, estimating the drag forced on droplets through the gas flow field should be considered. It is also crucial to observe the drag force exerted on the droplets in downstream of spray and after jet breakup initiation. Comparisons of the present model predictions with the experimental measurements have been carried out with two different nozzles for considerably different geometries. It is observed that a satisfactory agreement is achieved between the predicted droplet size and velocity distributions and experimental measurements in both initiation and downstream of the jet breakup region. Therefore, the present model may be applied to obtain the initial droplet size and velocity distributions for a wide variety of practical sprays.

Acknowledgements

Authors are grateful to C. P. Chen for carefully reading the manuscript and helpful remarks. Support from Tarbiat Modares University and Chemical and Material Department in UA Huntsville are acknowledged.

References and Notes

1. Jones, W.P.; Sheen, D.H. A probability density function method for modelling liquid fuel sprays. *Flow Turbul. Combust.* **1999**, *63*, 379-394.
2. Fritsching, U. *Spray Simulation*; Cambridge University Press: Cambridge, UK, 2004.
3. Chen, C.P.; Shang, H.M.; Jiang, Y. An efficient pressure-velocity coupling method for two-phase gas-droplet flows. *Int. J. Numer. Method Fluids* **1992**, *15*, 233-245.
4. Babinsky, E.; Sojka, P.E. Modeling droplet size distributions. *Prog. Energ. Combust. Sci.* **2002**, *28*, 303-329.
5. Lefebvre, A.H. *Atomization and Sprays*; Taylor & Francis: New York, NY, USA, 1989.
6. Liu, H.F.; Gong, X.; Li, W.F.; Wang, F.C.; Yu, Z.H. Prediction of droplet size distribution in spray of prefilming air-blast atomizers. *Chem. Eng. Sci.* **2006**, *61*, 1741-1747.

7. Sellens, R.W.; Brzustowski, T.A. A prediction of drop-size distribution in a spray from first principles. *Atomization Spray Tech.* **1985**, *1*, 89-102.
8. Li, X.; Tankin, R.S. Derivation of droplet size distribution in sprays by using information theory. *Combust. Sci. Technol.* **1987**, *60*, 345-357.
9. Ahmadi, M.; Sellens, R.W. A simplified maximum entropy based drop size distribution. *Atomization Sprays* **1993**, *3*, 292-310.
10. Cousin, J.; Yoon, S.J.; Dumouchel, C. Coupling of classical linear theory and maximum entropy formalism for prediction of drop size distribution in sprays. *Atomization Sprays* **1996**, *6*, 601-622.
11. Sellens, R.W; Brzustowski, T.A. A simplified prediction of droplet velocity distribution in a spray. *Combust. Flame* **1986**, *65*, 273-279.
12. Li, X.; Chin, L.P.; Tankin, R.S.; Jackson, T.; Stutrud, J.; Switzer, G. Comparison between experiments and predictions based on maximum entropy for sprays from a pressure atomizer. *Combust. Flame* **1991**, *86*, 73-89.
13. Shannon, C.E.; Weaver, W. *The Mathematical Theory of Communication*; University of Illinois Press: Urbana, IL, USA, 1949.
14. Dumouchel, C. The maximum entropy formalism and the prediction of liquid spray drop-size distribution. *Entropy* **2009**, *11*, 713-747.
15. Dumouchel, C. A new formulation of the maximum entropy formalism to model liquid spray drop-size distribution. *Part. Part. Syst. Charact.* **2006**, *23*, 468-479.
16. Movahednejad, E. *Prediction of Size and Velocity Distribution of Droplets in Spray by Maximum Entropy Principle and Using Wave Instability and Turbulence Analysis*, PhD Thesis; Tarbiat Modares University: Tehran, Iran, 2010.
17. White, F.M. *Viscous Fluid Flow*, 2nd ed.; McGraw-Hill: New York, NY, USA, 1991.
18. Mitra, S.K. *Breakup Process of Plane Liquid Sheets and Prediction of Initial Droplet Size and Velocity Distributions*, PhD Thesis; University of Waterloo: Waterloo, ON, Canada, 2001.
19. Kim, W.T.; Mitra, S.K.; Li, X. A predictive model for the initial droplet size and velocity distributions in sprays and comparison with experiments. *Part. Part. Syst. Charact.* **2003**, *20*, 135-149.
20. Sirignano, W.A.; Mehring, C. Comments on Energy Conservation in Liquid-Stream Disintegration. In Proceedings of ICLASS, Pasadena, CA, USA, July 2000.
21. Clift, R.; Grace, J.R.; Weber, M.E. *Bubbles, Drops and Particles*; Academic Press: New York, NY, USA, 1978.
22. Eberhart, C.J.; Lineberry, D.M.; Moser, M.D. Experimental Cold Flow Characterization of a Swirl Coaxial Injector Element. In Proceedings of 45th AIAA/ASME/SAE Joint Propulsion Conference, AIAA 2009-5140, Denver, CO, USA, August 2009.
23. Ommi, F.; Movahednejad, E.; Hosseinalipour, S.M.; Chen, C.P. Prediction of Droplet Size and Velocity Distribution in Spray Using Maximum Entropy Method. In proceedings of the ASME Fluids Engineering Division, FEDSM2009-78535, Vail, CO, USA, August 2009.